Human Ancestors Interbred with Two Distinct Populations of Distant Relatives

Alan R. Rogers Md Touhidul Islam Colin M. Brand Timothy H. Webster

March 22, 2026

Abstract

Ancient DNA has shown that a distantly-related "superarchaic" population interbred first with the ancestors of Neanderthals and Denisovans and later with Denisovans themselves. Other work has shown that a superarchaic population interbred with the African ancestors of all modern humans. But it is not yet clear whether these events involved the same superarchaic population. Here, we use the distribution of derived alleles among populations to evaluate hypotheses about superarchaics and their relationship to other hominins of the Pleistocene and Holocene. We find evidence for at least two distinct superarchaic populations. The one contributing to archaic Eurasian populations (Denisovans and Neanderthal-Denisovan ancestors) diverged earlier from the human lineage than did the one contributing to early moderns in Africa. These findings reveal previously unrecognized structure among hominin populations of the Pleistocene.

Introduction

The past 15 years have revolutionized our understanding of interbreeding between ancient populations. There was interbreeding not only between different groups of modern humans, but also between moderns and archaic populations of Neanderthals and Denisovans. Interbreeding was documented not only in Eurasia, but also in African populations, where the source population was often obscure[8,16,19]. There was also interbreeding between Eurasian archaic populations and a distantly-related population, which diverged early in the Pleistocene[30,31]. Because this population diverged earlier than did archaics, it has been called "superarchaic"[21]. There is evidence for superarchaic gene flow into Denisovans[13,21,22], into Neanderthal-Denisovan ancestors[27], and into Africans[4]. More recently, several publications have argued that early modern humans were a mixed population that received a substantial fraction of ancestry from a superarchaic population that separated from the modern-archaic trunk over a million years ago[3,7,23].

It is not yet clear whether there was one superarchaic population or several. Did the same superarchaic population contribute genes not only to archaic Eurasian populations but also to African ones? Or were there multiple superarchaic populations? In what follows, we present evidence for the second of these alternatives. We show that there were at least two superarchaic populations. The one that diverged first contributed ancestry to archaic Eurasian populations. The other contributed to the African ancestors of modern humans.

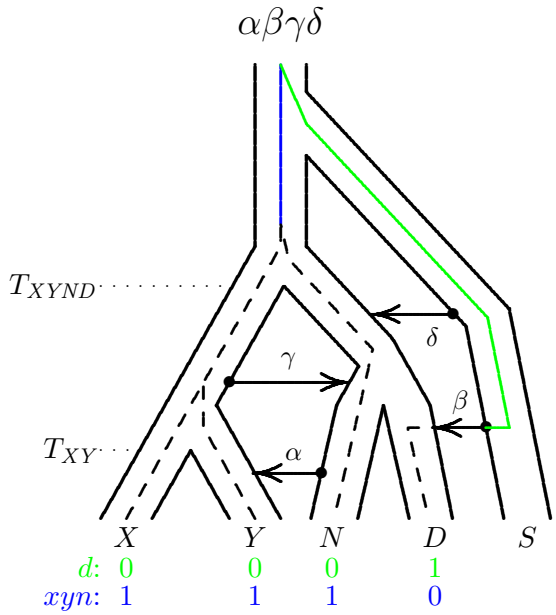

Figure 1: Model of population history proposed in 2020[27]. Greek letters are episodes of gene flow; roman letters are populations: X, Africa; Y, Europe; N, Neanderthal; D, Denisovan; S, Superarchaic. T_{XY} is the separation time of X and Y, and T_{XYND} is that of XY (the population ancestral to X and Y) from ND (that ancestral to N and D). Internal lines show the gene genealogy of a single nucleotide site. A mutation on the green edge would generate site pattern d; one on blue would generate xyn.

Results

Comparing models of population history using nucleotide site patterns

Our notation is illustrated in Fig. 1, using a model proposed previously[27]. Capital letters refer to populations: X for west Africa, Y for Europe, N for Neanderthal, D for Denisovan, and S for superarchaic. Combinations of these letters refer to ancestral populations. For example, XY is the population ancestral to X and Y. Greek letters refer to episodes of admixture. The green, blue, and dotted lines indicate the gene genealogy of a hypothetical genetic locus at which we have observed one haploid sample each from populations X, Y, N, and D. Greek letters refer to episodes of gene flow. For example, α refers to $N \to Y$ gene flow—from population N into Y, and δ refers to $S \to ND$ gene flow. Combinations of Greek letters refer to models. For example, Fig. 1 illustrates model $\alpha\beta\gamma\delta$, which includes four episodes of gene flow: α, β, γ, and δ.

Our analysis involves the frequencies of *site patterns*, two of which are shown on the bottom of the graph. If a mutation occurred on the green branch, the sample from D would carry the derived allele ("1") at this locus, and the other samples would carry the ancestral allale ("0"). This configuration is called the "d site pattern" and is shown in green at the bottom of the graph. Similarly, a mutation on the blue branch would generate site pattern xyn, which is shown at the bottom in blue. The relative frequencies of site patterns can be estimated from data, and their expected values calculated using our *Legofit* software[25,26]. Legofit estimates parameters by minimizing the difference between observed and expected site pattern frequencies.

We used 12 published high-coverage genomes, which we grouped into 4 sets: X, 3 genomes from the modern Yoruba of west Africa[18]; Y, 5 from the modern French and English[18]; R, 2 Neanderthals

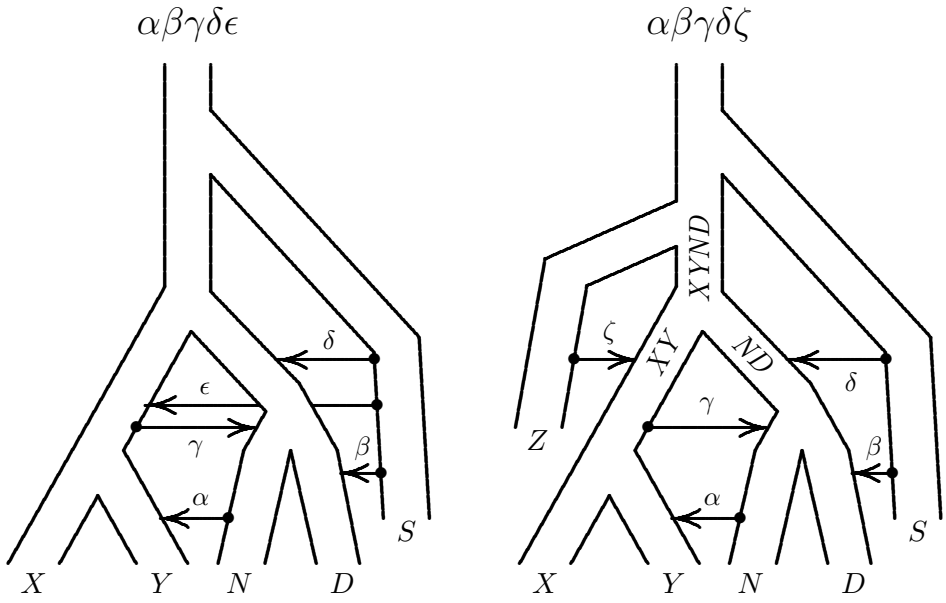

Figure 2: Two new models of population history with superarchaic admixture into the ancestors of modern humans. On the right, Z is a superarchaic population that diverged more recently than S and contributed ancestry (ζ) to ancestral moderns. XY, ND, and $XYND$ label ancestral populations.

(Chagyrskaya[17] and Vindija[22]); A, 1 older Neanderthal (Altai[21]); and D, Denisovan[24]. Site patterns are labeled with combinations of these letters in lower case.

Fig. 2 shows the two most complex models considered in the current analysis. On the left, model $\alpha\beta\gamma\delta\epsilon$ adds one episode of gene flow to the previous model (Fig. 1). In this episode, ϵ, early modern humans (XY) receive gene flow from the same superarchaic population that contributed to Denisovans and to the ancestors of Neanderthals and Denisovans. The model on the right ($\alpha\beta\gamma\delta\zeta$) also assumes that XY receives gene flow, but in this case the source is a distinct superarchaic population, Z, which diverged from the trunk more recently than S. In addition to these complex models, we also considered several simpler ones, which omit one or more episodes of gene flow.

Evidence for two distinct superarchaic populations

Our statistical analysis supports model $\alpha\beta\gamma\delta\zeta$, in which there are two distinct populations of superarchaics, one contributing to archaics and another contributing to the ancestors of modern humans. This conclusion rests on the "bootstrap estimate of predictive error" (bepe), a statistical method for choosing among models[5,6]. Bepe uses the real data to estimate parameters and calculate expected site-pattern frequencies. It then compares these expectations to site-pattern frequencies in all 50 replicates produced by a moving-blocks bootstrap[15]. Bepe is the mean squared difference between predicted frequencies and those observed in bootstrap replicates (plus a correction for bootstrap bias). The preferred model is the one whose bepe value is lowest. In table 1, the preferred model is $\alpha\beta\gamma\delta\zeta$, but the other bepe values are also small. The question thus arises, how strongly should we weight the preferred model?

The support for model $\alpha\beta\gamma\delta\zeta$ is strong. This conclusion rests on the method of "bootstrap model averaging"[1] (booma). Booma iterates across all 51 data sets (the real data and 50 bootstrap replicates), pretends temporarily that the current data set is real and the others are bootstrap replicates, and calculates bepe for all models. The booma weight of each model is the fraction

Table 1: Bootstrap estimate of predictive error (bepe) values and bootstrap model average (booma) weights

Model	bepe	weight
$\alpha\beta\gamma$	2.17×10^{-7}	0
$\alpha\beta\delta$	1.62×10^{-7}	0
$\alpha\gamma\delta$	4.94×10^{-7}	0
$\beta\gamma\delta$	6.06×10^{-7}	0
$\alpha\beta\gamma\delta$	2.85×10^{-7}	0
$\alpha\beta\gamma\zeta$	1.71×10^{-7}	0.02
$\alpha\beta\delta\zeta$	1.84×10^{-7}	0
$\alpha\gamma\delta\zeta$	2.62×10^{-7}	0
$\alpha\beta\gamma\delta\epsilon$	1.46×10^{-7}	0
$\alpha\beta\gamma\delta\zeta$	1.35×10^{-7}	0.98

of these contests that it wins, i.e. the fraction in which its bepe value is lowest. Table 1 shows that model $\alpha\beta\gamma\delta\zeta$ gets the preponderance of the booma weight. One other model gets 2% of the weight, and the rest get 0. Bootstrap replicates approximate repeated samples from the process that created the data. Consequently, these results imply that the advantage of the preferred model is large compared with variation in repeated sampling.

Of the two models in Fig. 2, the one on the left gets 0 weight, whereas the one on the right gets 98%. This is strong evidence that early modern humans received gene flow from a distinct superarchaic population—not from the one that contributed to Denisovans (episode β) and to the ancestors of Neanderthals and Denisovans (δ).

After fitting the preferred model, $\alpha\beta\gamma\delta\zeta$, the residual errors are generally small, as shown in Fig. 3. Nonetheless, several of them deviate significantly from 0, suggesting that the model is not yet a perfect fit. On the other hand, we don't expect a perfect fit—any effort to select models by minimizing residuals would result in overfitting.

Model-averaged parameter estimates (Fig. 4) are in general agreement with previous work[27], but there are a few exceptions. $\hat{m}_\gamma$ has changed from 0.016 to 0.045, implying more gene flow from early moderns into Neanderthals. $\hat{m}_\delta$ has changed from 0.034 to 0.058, implying more gene flow from Asian superarchaics into the Neanderthal-Denisovan ancestors. $\hat{N}_S$ has changed from 27 k to 2.4 M, implying a larger size or deeper subdivision within the population of Asian superarchaics.

Although many of the confidence intervals in Fig. 4 are narrow, some are quite large, and several of these large intervals reflect identifiability problems. For example, supplementary Fig. S3 shows that estimates of N_Z and N_B cluster tightly along a straight line with positive slope. This implies that composite likelihood depends on these parameters primarily through their difference, so that an increase in one parameter can be offset by an increase in the other.

Identifiability problems such as these can underlie not only wide confidence intervals but also bias. Our legofit analysis may have additional bias, because it ignores states with probability less than 10^{-6}, as discussed below. To measure these biases, we analyzed 50 data sets simulated with msprime[11] under the preferred model, $\alpha\beta\gamma\delta\zeta$. Fig. 5 shows the results. In this figure, red crosses are true parameters values used as input by the simulation, and blue circles are legofit estimates. Admixture and time parameters show little bias, although there is substantial variation among estimates of m_ζ and T_{XY}. Among population size parameters with large values (N_B, N_Z, and N_S) most estimates are larger than the true values, indicating an upward bias. These parameters describe the sizes of the early Neanderthal population and of the two superarchaic populations.

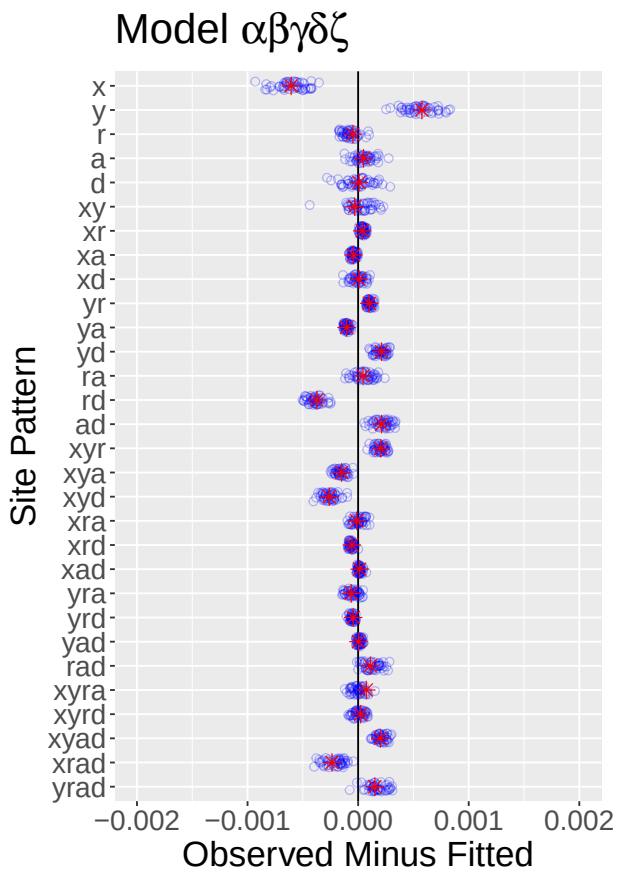

Figure 3: Residual errors in real data (red asterisks) and bootstrap replicates (blue circles)

Consequently, the estimates in Fig. 4 may be too large. Among size parameters with smaller values (N_N, N_{XY}, N_{ND}, and N_{XYND}), the opposite is true—estimates are biased downward, and the real estimates in Fig. 4 are probably too small. In spite of these problems, these results show that in most cases, the true values are either close to their estimates or are surrounded by a relatively unbiased swarm. Thus, the simulations show that legofit does a reasonable job of estimating this model.

Discussion

These results solve a puzzle: under model $\alpha\beta\gamma\delta$[27] (Fig. 1), successive methodological improvements led to less and less plausible estimates of the separation time, T_{XY}, between modern west Africans and Europeans. This separation probably happened about 50 ka ago, a date supported both by archaelogical and genetic data[12,28]. Our first estimate of this parameter (row 1, supplementary table S2) is consistent with this consensus. The table's second row differs from the first only in using a more accurate algorithm[26]. The third row adds an additional archaic genome[17]. With each improvement, the estimate of T_{XY} becomes less plausible. By row 3 it has become absurd, implying that Europeans and Africans separated only a few thousand years ago. This suggests that the model is misspecified, resulting in a bias that becomes clearer with greater accuracy and more data.

This bias arises because Africans and Europeans uniquely share more derived alleles than model

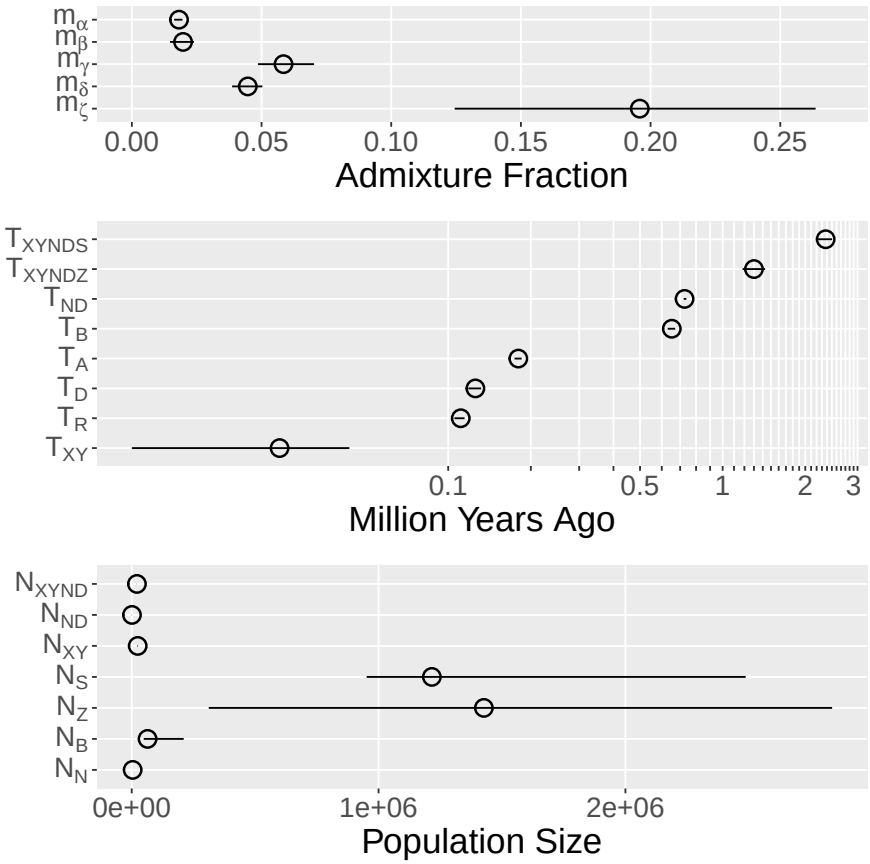

Figure 4: Model-averaged parameter estimates and confidence intervals estimated by moving-blocks bootstrap[15]. Admixture fractions: m_i, fraction of recipient population derived from donor during admixture episode i. Time parameters: T_{XYNDS}, separation time of S from the ancestors of X, Y, N, and D; T_{XYNDZ}, separation time of Z from the ancestors of X, Y, N, and D; T_{ND}, separation time of N and D; T_B, time at which the Neanderthal population changed size; T_A, age of the Altai Neanderthal; T_D, age of the Denisovan genome; T_R, average age of the Chagyrskaya and Vindija Neanderthals; T_{XY}, separation time of X and Y. Effective population sizes: N_{XYND}, size of population ancestral to X, Y, N, and D; N_{ND}; size of population ancestral to N and D; N_{XY}, size of population ancestral to X and Y; N_S, size of population S; N_Z, size of population Z; N_B, of early Neanderthal population; N_N, size of later Neanderthal population.

$\alpha\beta\gamma\delta$ can easily accomodate. In response, the optimization algorithm wants to increase the length of the branch ancestral to west Africans and Eurasians in the population tree. In principal, it could do so either by (1) increasing the separation time, T_{XYND}, of moderns and archaics, or by (2) reducing the separation time, T_{XY}, of Eurasians and Africans. (These parameters are illustrated in Fig. 1.) Option 1 is unavailable however because T_{XYND} has a fixed value that is used to calibrate the molecular clock. Thus, only T_{XY} is free to vary, and the optimizer has pushed it to an implausibly low value. The present results resolve this discrepancy. In the model-averaged estimates, the upper end of the T_{XY} confidence interval is about 44 ka, which is not far short of accepted views about the separation time of Europeans and west Africans.

Our results agree with several recent publications[3,7,32], which find that the early modern human population (XY in the right panel of Fig. 2) received substantial gene flow from a superarchaic

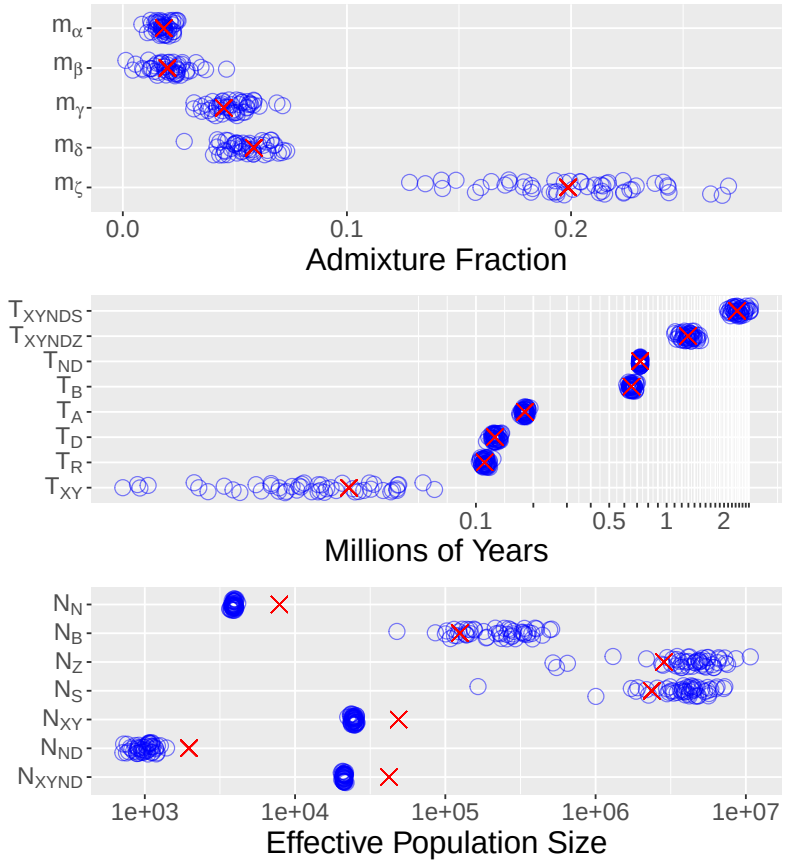

Figure 5: Estimates from simulations of the fitted model. Blue circles show estimates based 50 data sets simulated with msprime[11]. Red crosses show true parameter values. Parameters are defined in the caption of Fig. 4.

population (our Z) that diverged prior to the separation of archaics from the ancestors of moderns. Population Z separated from *XYND* 1–3 Ma ago in the reconstruction of Fan et al.[7], ∼1.5 Ma in that of Cousins et al.[3], over 500 ka in that of Zhang et al.[32] and 1.3 Ma (95% CI: 1.181–1.428) in ours, assuming generations of 29 y. The contribution of population Z is 5–15% for Fan et al., 21% for Cousins et al., 0.5–1.1% for Zhang et al., and 19.6% (95% CI: 12.4–26.4%) for us.

In another recent study, Ragsdale et al.[23] agree that early modern humans were a mixture and that the population contributing the majority to this mixture is related to Neanderthals and Denisovans. But they find that the fit is improved if continuous gene flow is allowed between the two populations contributing to this mixture. Perhaps because of this gene flow, their estimate of the separation time is larger—about 1.7 Ma ago.

The similarity between these sets of findings is remarkable in view of the differences between methods. Some of the methods ignore linkage disequilibrium whereas others rely on it. Some use variation within populations (or even within individuals) whereas others use differences between populations. Yet the studies reach similar conclusions and are thus mutually supportive.

Our own study is unique in showing that archaics and moderns interbred with two distinct superarchaic populations—one contributing to archaics and another to early moderns. This new finding requires revision of our previous views about the Middle Pleistocene. In an earlier publication[27], we found that the ancestors of Neanderthals and Denisovans interbred with the same

superarchaic population that later interbred with Denisovans. To make sense of this, we pointed out that the first wave of emigration out of Africa happened early in the Pleistocene, when *Homo erectus* spread across Eurasia. Later, during the Middle Pleistocene, humans evolved larger brains and began making Acheulean tools. Both of these innovations appear in Africa before Eurasia, suggesting a second wave of emigration out of Africa[9,10]. We proposed[27] that this second wave interbred with the Eurasian descendants of the first, during what we refer to as the δ episode of admixture. It seemed plausible that, before this contact, the two populations had remained largely isolated because of the difficulty of traveling between Africa and Eurasia. (At least during the Upper Pleistocene, human contact between these continents was largely restricted to relatively brief periods when the Sahara was humid[2].)

Now we have evidence of a second superarchaic population, Z, which diverged after the first and later interbred with the ancestors of modern humans. This contact presumably occurred in Africa, because it happened before moderns spread into Eurasia. We considered the possibility that this second superarchaic population was the same as the first—see model $\alpha\beta\gamma\delta\epsilon$ in Fig. 2—but that model fared poorly (table 1). Thus, there were two superarchaic populations, and it seems likely that the second (population Z) was African.

This is puzzling, because it implies that two African populations—population Z and the ancestors of moderns, Neanderthals, and Denisovans—remained essentially isolated across roughly a million years. What kept them apart? Africa has no mountain barriers as large as the Himalayas or the Alps. There are deserts, but these were not continuously arid[29]. The results of Ragsdale et al.[23] (see above) suggest that these populations may not have been isolated after all—perhaps there was a continuous trickle of gene flow between them. Yet somehow (as discussed above) population Z acquired many mutations that show up in modern humans but not in Neanderthals and Denisovans. If there was gene flow between these populations, it must have been weak.

Methods

We used 12 published high-coverage genomes. The population X sample consists of the 3 Yoruban genomes published by the Simons Genome Diversity Project[18] (SGDP). The Y sample consists all 3 French and both English samples in the SGDP. The R sample consists of 2 relatively recent Neanderthal genomes: Vindija[22] and Chagyrskaya[17]. The A sample is the Altai Neanderthal genome[21]). The D sample is the high-coverage Denisovan genome[24].

All genomes were downloaded from the websites of the SGDP and the Max Planck Institute for Evolutionary Anthropology. Methods for quality control, calling ancestral alleles, and calibrating the molecular clock are as described by Rogers et al.[27].

Legofit[25,26] estimates parameters by minimizing the Kullback-Leibler divergence[14] (KL) between observed and expected site-pattern frequencies. Its minimization engine uses the differential evolution[20] (DE) algorithm, which maintains a swarm of points—10 times as many as there are parameters—each of which represents a set of guesses about all free parameters. In each iteration, the points with lowest KL divergence mutate, recombine, and reproduce to form the next generation of points.

Our Legofit analysis involves four stages. The first two are very fast and achieve only an approximate fit. Then principal components (PC) analysis is used to reduce the number of parameters and to re-express free variables on orthogonal coordinates. Finally, legofit's deterministic algorithm provides a more accurate fit. Analysis of most models was as follows:

1. Stage a1 used legofit's stochastic algorithm with arguments `--tol 3e-5 -S 100@1000 -S 1000@10000`. This says that the tolerance criterion is 3e-5, which is fairly large and means

that the DE iterations will stop when the fit is only fair. The other arguments say that we start with 100 DE iterations in each of which the objective function is estimated from 1000 simulation replicates. Then it does 1000 DE iterations with 10000 replicates per function evaluation.

2. Stage a2 also uses stochastic algorithm and uses the same `--tol` value as a1. It initializes the DE algorithm with points sampled from the point swarms of all data sets (real data and bootstrap replicates) in stage a1. In this stage, legofit does at most 500 DE iterations with 10000 replicates per function evaluation.

3. Stages b1 and b2 operate on principal components (PCs) rather than on the original variables. PCs that account for less than a fraction 0.001 of the total variance are ignored. Stage b2 also does 500 DE iterations of the stochastic algorithm with 10000 replicates per function evaluation.

4. Stage b2 initializes the DE algorithm by sampling from the point swarms of all data sets in stage b1. It uses the deterministic algorithm with argument `-d 1e-6`, which says to ignore states with probability less then 1e-6. Without this approximation, the deterministic algorithm would be not be feasible with our most complex models. The summed probability of ignored events was a fraction 0.0008 of the total probability. The tolerance criterion is dropped to 3e-6 for this final stage and there are 2000 DE iterations. In no case did the algorithm go the full 2000 iterations. It always stopped early because it had reached the tolerance criterion.

We don't estimate the timing of admixture events, because most of the information about these parameters is in linkage disequilibrium, which our method ignores. Because our method is insensitive to these parameters, we constrain their values to arbitrary time points within the relevant interval. For example, T_β is constrained to equal $(T_D + T_{ND})/2$. Some episodes of admixture (α and β) affect only one sampled genome. For these episodes, the timing of admixture has no effect on likelihood, and we lose nothing by fixing the values of these parameters. The other episodes (γ, δ, and ζ) affect more than one sampled genome, and for these our approach is an approximation.

In some of the smaller models ($\alpha\beta\gamma$, $\alpha\beta\delta$, $\alpha\gamma\delta$, $\beta\gamma\delta$), which were done early in the project, we used the derministic algorithm with `-d 0`. This does not ignore events of low probability and thus makes the calculations more accurate. Ordinarily we wouldn't compare models fit using different values of the `-d` parameter, because smaller values provide greater accuracy and give the model an advantage in model selection. But since these small models were all excluded in model selection, we did not re-run these models using the same parameters used for the large ones.

Acknowledgements

This work was supported by NSF BCS 1945782 (ARR and TWH) and the Center for High Performance Computing at the University of Utah (ARR). All scripts and pipelines are available at `XXXXXX`.

Author contributions

ARR developed the Legofit software, did Legofit analyses, and wrote the manuscript. MTI did Legofit analyses. All authors collaborated on study design, interpretation, and manuscript revision.

References

1. Buckland, S. T., Burnham, K. P. & Augustin, N. H. (1997). Model Selection: an Integral Part of Inference. *Biometrics* **53,** 603–618.
2. Castañeda, I. S. *et al.* (2009). Wet Phases in the Sahara/Sahel Region and Human Migration Patterns in North Africa. *Proceedings of the National Academy of Sciences, USA* **106,** 20159–20163.
3. Cousins, T., Scally, A. & Durbin, R. (Apr. 2025). A Structured Coalescent Model Reveals Deep Ancestral Structure Shared by All Modern Humans. *Nature Genetics* **57,** 856–864.
4. Durvasula, A. & Sankararaman, S. (2020). Recovering Signals of Ghost Archaic Introgression in African Populations. *Science Advances* **6,** aax5097.
5. Efron, B. (1983). Estimating the Error Rate of a Prediction Rule: Improvement on Cross-Validation. *Journal of the American Statistical Association* **78,** 316–331.
6. Efron, B. & Tibshirani, R. J. (1993). *An Introduction to the Bootstrap* (Chapman and Hall, New York, 1993).
7. Fan, S. *et al.* (2023). Whole-Genome Sequencing Reveals a Complex African Population Demographic History and Signatures of Local Adaptation. *Cell* **186,** 923–939.
8. Hsieh, P. *et al.* (2016). Model-Based Analyses of Whole-Genome Data Reveal a Complex Evolutionary History Involving Archaic Introgression in Central African Pygmies. *Genome Research* **26,** 291–300.
9. Hublin, J.-J. (1998). In *Neandertals and Modern Humans in Western Asia* (eds Akazawa, T., Aoki, K. & Bar-Yosef, O.) 295–310 (Kluwer, 1998).
10. Hublin, J.-J. (2009). The Origin of Neandertals. *Proceedings of the National Academy of Sciences, USA* **106,** 16022–16027.
11. Kelleher, J., Etheridge, A. M. & McVean, G. (May 2016). Efficient Coalescent Simulation and Genealogical Analysis for Large Sample Sizes. *PLoS Computational Biology* **12,** 1–22.
12. Kerdoncuff, E. *et al.* (June 2025). 50,000 Years of Evolutionary History of India: Impact on Health and Disease Variation. *Cell* **188,** 3389–3404.e6.
13. Kuhlwilm, M. *et al.* (Feb. 2016). Ancient Gene Flow from Early Modern Humans into Eastern Neanderthals. *Nature* **530,** 429–433. ISSN: 1476-4687.
14. Kullback, S. & Leibler, R. A. (Mar. 1951). On Information and Sufficiency. *The Annals of Mathematical Statistics* **22,** 79–86.
15. Liu, R. Y. & Singh, K. (1992). In *Exploring the "Limits" of the Bootstrap* (eds LePage, R. & Billard, L.) 225–248 (Wiley, New York, 1992).
16. Lorente-Galdos, B. *et al.* (2019). Whole-genome Sequence Analysis of a Pan African Set of Samples Reveals Archaic Gene Flow from an Extinct Basal Population of Modern Humans into Sub-Saharan Populations. *Genome Biology* **20,** 77.
17. Mafessoni, F. *et al.* (2020). A High-Coverage Neandertal Genome from Chagyrskaya Cave. *Proceedings of the National Academy of Sciences, USA* **117,** 15132–15136.
18. Mallick, S. *et al.* (2016). The Simons Genome Diversity Project: 300 Genomes from 142 Diverse Populations. *Nature* **538,** 201–206. ISSN: 1476-4687.
19. Plagnol, V. & Wall, J. D. (2006). Possible Ancestral Structure in Human Populations. *PLoS Genetics* **2,** e105.

20. Price, K., Storn, R. M. & Lampinen, J. A. (2006). *Differential Evolution: A Practical Approach to Global Optimization* ISBN: 978-3-540-20950-8 (Springer Science and Business Media, Berlin, 2006).

21. Prüfer, K. *et al.* (2014). The Complete Genome Sequence of a Neanderthal from the Altai Mountains. *Nature* **505,** 43–49.

22. Prüfer, K. *et al.* (2017). A High-Coverage Neandertal Genome from Vindija Cave in Croatia. *Science* **358,** 655–658.

23. Ragsdale, A. P. *et al.* (May 2023). A Weakly Structured Stem for Human Origins in Africa. *Nature* **617,** 755–763.

24. Reich, D. *et al.* (2010). Genetic History of an Archaic Hominin Group from Denisova Cave in Siberia. *Nature* **468,** 1053–1060.

25. Rogers, A. R. (2019). Legofit: Estimating Population History from Genetic Data. *BMC Bioinformatics* **20,** 526.

26. Rogers, A. R. (2022). An Efficient Algorithm for Estimating Population History from Genetic Data. *Peer Community Journal* **2,** e32.

27. Rogers, A. R., Harris, N. S. & Achenbach, A. A. (2020). Neanderthal-Denisovan Ancestors Interbred with a Distantly-Related Hominin. *Science Advances* **6,** eaay5483.

28. Sümer, A. P. *et al.* (Feb. 2025). Earliest Modern Human Genomes Constrain Timing of Neanderthal Admixture. *Nature* **638,** 711–717.

29. Von der Meden, J. *et al.* (2022). Tufas Indicate Prolonged Periods of Water Availability Linked to Human Occupation in the Southern Kalahari. *PLoS ONE* **17,** e0270104.

30. Waddell, P. J. (2013). Happy New Year *Homo erectus*? More Evidence for Interbreeding with Archaics Predating the Modern Human/Neanderthal Split. *ArXiv* **1312.7749.**

31. Waddell, P. J., Ramos, J. & Tan, X. (2011). *Homo denisova*, Correspondence Spectral Analysis, Finite Sites Reticulate Hierarchical Coalescent Models and the Ron Jeremy Hypothesis. *ArXiv* **1112.6424.** eprint: `1112.6424`.

32. Zhang, Y., Biddanda, A., Johnson, S. A., O'Dushlaine, C. & Moorjani, P. (2026). Recovering Signatures of Archaic Introgression using Ancestral Recombination Graphs. *bioRxiv.*